THE ASTROPHYSICAL JOURNAL, 523:L181–L184, 1999 October 1

MIGRATION OF ZONAL FLOWS DETECTED USING MICHELSON DOPPLER IMAGER *f*-MODE FREQUENCY SPLITTINGS

J. SCHOU
Center for Space Science and Astrophysics, HEPL Annex A201, Stanford University, Stanford, CA 94305-4085; jschou@solar.stanford.edu
Received 1999 July 7; accepted 1999 August 4; published 1999 August 26

ABSTRACT

The small-scale zonal flows in the outer part of the solar convection zone were recently detected by Kosovichev & Schou using *f*-mode frequency splittings. Results from five 72 day time series (Schou et al.) show a slight drift of the pattern toward the equator in a manner similar to that seen in the so-called torsional oscillation observed using surface Doppler shift measurements. Here I describe results using 12 72 day time series of the Michelson Doppler Imager medium-*l* data. These results show a clear drift of the pattern toward the equator. Also, the near-surface rotation rate close to the solar poles is observed to be slower than expected from an extrapolation from lower latitudes and to be changing with time.

Subject headings: Sun: activity — Sun: interior — Sun: oscillations — Sun: rotation

1. INTRODUCTION

Small-scale zonal flows were initially observed in surface Doppler shift data (Howard & LaBonte 1980). These so-called "torsional oscillations" appear as bands of slightly faster and slower rotation. It has been noticed that these bands migrate toward the equator in a manner similar to the bands of solar activity (as illustrated by the butterfly diagram). However, while theories have been proposed to explain the origin of these flows and their relationship to the activity, there has been a lack of observational data beyond the surface measurements. It has even been suggested that the bands may be an artifact of the way the Doppler shift measurements are made.

Using helioseismic techniques, these flows have recently been measured in the outer parts of the convection zone (Kosovichev & Schou 1997; Schou et al. 1998a, 1998b; Birch & Kosovichev 1998a, 1998b). Helioseismic measurements, unlike the Doppler measurements, allow us to get an idea of the subsurface structure of the flows and to probe closer to the solar poles where foreshortening makes surface measurements difficult. Also, they serve as an independent test verifying the surface measurements made over the last two decades, allowing us to study those with more confidence.

2. DATA ANALYSIS AND RESULTS

The results presented here cover 12 72 day time series obtained with the Michelson Doppler Imager (MDI) instrument on the *Solar and Heliospheric Observatory* (*SOHO*) spacecraft. The results are from the so-called medium-*l* program that provides almost continuous coverage. In the medium-*l* program, the original Dopplergrams are convolved with a Gaussian and subsampled on a 200 × 200 grid, thus limiting the coverage to modes with degree $l \leq 300$. The first 11 of these time series represent essentially all the usable data between the start of the mission and the interruption due to spacecraft problems in mid-1998. The nominal start time of the first series is 1996 May 1, and the nominal end time of the last of the 11 series is 1998 July 1. The final series was taken after the recovery of the spacecraft and nominally covers the time period 1999 February 3 through 1999 April 15. For some of the series (such as the first and those around the interruption), the actual times are different by up to a few days.

The first step in the analysis is to perform a spherical harmonic transform. For the medium-*l* data, modes with l up to 300 are used. Next, mode parameters are determined from each 72 day time interval and each mode, using the method described in Schou (1992). Rather than determining individual mode frequencies ν_{nlm}, where n is the radial order of the mode and m the azimuthal order, so-called *a*-coefficients are used. These *a*-coefficients are the coefficients in a polynomial expansion

$$\nu_{nlm} = \nu_{nl} + \sum_{j=1}^{j_{\max}} a_j(n, l)\mathcal{P}_j^{(l)}(m),$$

where ν_{nl} is the mean multiplet frequency and the $\mathcal{P}$'s are orthogonal polynomials of degree l (Schou, Christensen-Dalsgaard, & Thompson 1994).

For the present work, only the *f*-mode is used, and the fit is done using $j_{\max} = 36$ *a*-coefficients. Given the extremely long lifetime of the *f*-modes, their frequencies can be determined very accurately, and they are less likely to suffer from a number of possible systematic errors. In particular, the spacings between a mode and the leaks from adjacent degrees are large relative to the line width, thus minimizing any errors resulting from problems with the leakage calculations.

The *f*-modes used here sample a region very close to the surface, as illustrated in Figure 1, and for the purpose of this Letter, it is assumed that the rotation rate is independent of radius r in the Sun within this region, at least for the small-scale structure (as was shown in Schou et al. 1998b). Under this assumption, it may be shown (Pijpers 1997) that coefficients c_{ls} and kernels K_s exist such that

$$2\pi a_{2s+1}(n, l) = c_{ls} \int_0^1 K_s(x)\Omega(x)dx,$$

where Ω is the north-south symmetric component of the solar rotation rate, $x = \cos\theta$, and θ is the colatitude. As shown in

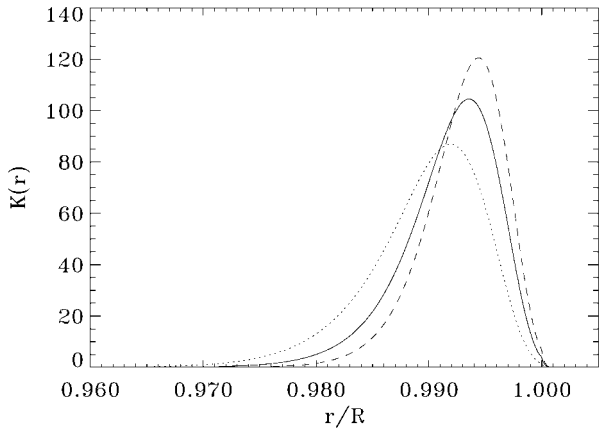

FIG. 1.—Radial kernels. The dotted line shows a mode kernel for $l = 160$, the dashed line a kernel for $l = 250$, and the solid line the average of the kernels for the modes used. The center of gravity of the average kernels is at $r/R = 0.9917$.

Pijpers (1997), the dominant variation with l of c_{ls} is given by

$$v_{2s+1}^{(l)} = \frac{(-1)^s(2l+1)!(2s+2)!(l+s+1)!}{ls!(s+1)!(l-s-1)!(2l+2s+2)!}.$$

The l-dependent part of this is given by

$$c'_{ls} = 2^{2s+1}\frac{1}{l}\frac{(2l+1)!(l+s+1)!}{(l-s-1)!(2l+2s+2)!},$$

where the factor 2^{2s+1} is included to make the correction unity in the high-l limit. A simple analysis shows that

$$c'_{ls} \approx e^{-s(s+3/2)/l}$$

to a very good approximation. To a good approximation, we therefore have

$$2\pi a'_{2s+1}(n, l) = \int_0^1 K_s(x)\Omega(x)dx,$$

where $a'_{2s+1}(n, l) = a_{2s+1}(n, l)/c'_{ls}$.

It follows from what has preceded that the modified a-coefficients a' (which in the rest of the Letter will be referred to without the prime symbol) should not depend on l if there are no radial variations, as is observed in the splittings, making it possible to average the coefficients over l. For the results presented here, the averaging is done over the available modes in the interval $160 \le l \le 250$. Unfortunately, not all modes are available for all time intervals, and so between 67 and 79 out of a possible 91 modes are used. Given the lack of trends with l, this should not cause significant problems. The resulting l-averaged splittings are shown in Figure 2, and the resulting radial sensitivity are shown in Figure 1. With the notable exception of a_1 (which is related to the angular momentum), most of the coefficients vary systematically during this time period.

The final step in the analysis is to invert the splittings in order to infer an estimate of the rotation rate as a function of latitude. In Kosovichev & Schou (1997), this was done by expanding Ω in a polynomial in x^2 with the same number ($j_{\max}/2 = 18$) of terms as there are a-coefficients and solving for the coefficients in the polynomial. In this Letter, a multiplicative optimally localized average (MOLA; see, e.g., Christensen-Dalsgaard, Schou, & Thompson 1990; Schou et al. 1998b) technique is used. For any linear inversion method, the solution at a target point x_0 can be written as

$$\bar{\Omega}(x_0) = \sum_{s=0}^{s_{\max}} c_s(x_0)a_{2s+1} = \sum_{s=0}^{s_{\max}} c_s(x_0)\int_0^1 K_s(x)\Omega(x)dx = \int_0^1 K(x_0, x)\Omega(x)dx,$$

where $s_{\max} = j_{\max}/2 - 1$, and

$$K(x_0, x) = \sum_{s=0}^{s_{\max}} c_s(x_0)K_s(x)$$

is a so-called averaging kernel. Also, the standard deviation on the inferred rotation rate can be estimated as

$$\sigma[\bar{\Omega}(r_0)]^2 = \sum_{s=0}^{s_{\max}} c_s(x_0)^2\sigma_{2s+1}^2,$$

where σ_{2s+1} is the estimated standard error associated with a_{2s+1}. It is important to note that this is only the result of propagating the estimated errors on the input splittings. It should not be interpreted as an estimate of the difference between the true rotation rate at x_0 and the inferred rate. In particular, any small-scale structure will have been smeared out, as discussed in, e.g., Schou et al. (1998b).

The idea of the MOLA technique is to localize the averaging kernel close to the target point while controlling the errors on the inferred rotation rate. This is done by finding the coefficients $c_s(r_0)$ that minimize

$$\int_0^1 K(x_0, x)^2(x - x_0)^2dx + \mu\sum_{s=0}^{s_{\max}} c_s(x_0)^2\sigma_{2s+1}^2$$

subject to a unimodularity constraint

$$\int_0^1 K(x_0, x) = 1,$$

where μ is a trade-off parameter. The trade-off parameter μ determines the trade-off between getting localized information (the first term) and minimizing the noise contribution (the second term). Generally, there is a large number of observations, and the kernels are almost degenerate. In the present case, however, there are only 18 averaged a-coefficients, and the kernels are nondegenerate, and it turns out that $\mu = 0$ gives quite reasonable errors while achieving the best possible resolution. Results are shown in Figure 3. To show the small-scale zonal flows, the temporal average was subtracted from a_1 through a_5. This is equivalent to subtracting a second-order polynomial in $\cos^2(\theta)$, where θ is the colatitude, from the rotation rate (unlike Schou et al. 1998a where the lowest a-coefficients were simply set to zero). As shown by the av-

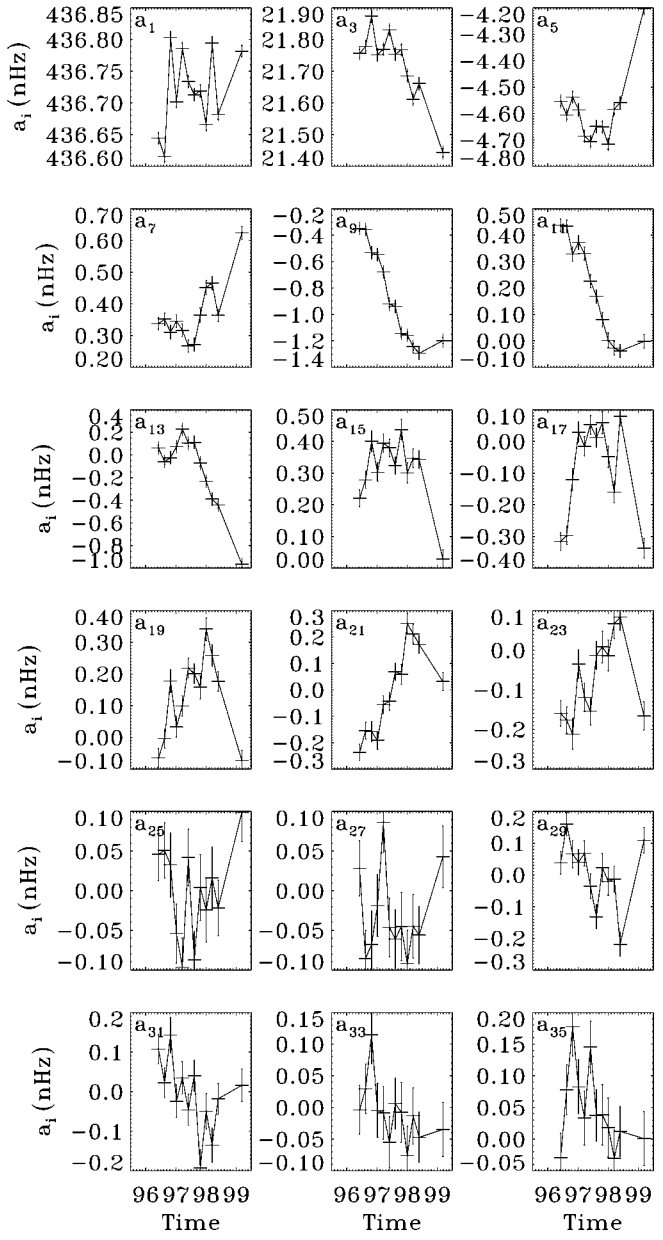

FIG. 2.—Averaged odd a-coefficients as a function of index and time. For each index (i), the a-coefficients are connected with lines illustrating their temporal change. Error bars are 1 σ. Only modes with $160 \le l \le 250$ were used, and the averaging was done over the available modes as described in the main text.

eraging kernels in Figure 4, the resolution in latitude is between 5° and 10°. Using a regularized least-squares (RLS) inversion method (Christensen-Dalsgaard et al. 1990; Schou et al. 1998b) gives results similar to those from the method of Kosovichev & Schou (1997) at low regularization and results more similar to the MOLA results when regularized harder. However, as has been observed before, the MOLA-averaging kernels, unlike the RLS kernels, tend to be positive, thereby, perhaps, making the interpretation easier. Also, the wider and positive kernels tend to suppress oscillations, making the estimates more conservative for the present purpose (looking for deviations from the three-term expansion).

The most striking features in Figure 3 are the small-scale patterns drifting toward the equator and the slow rotation rate

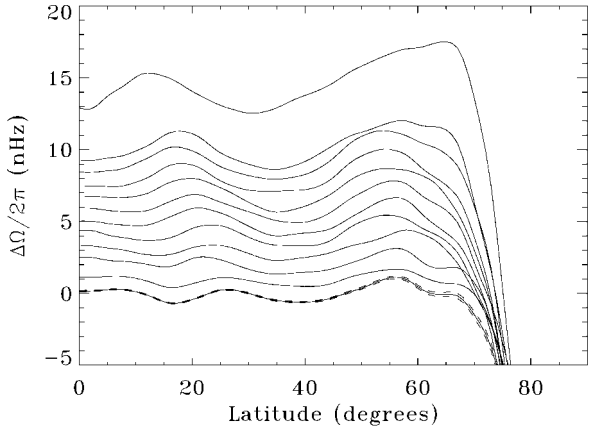

FIG. 3.—The zonal flows as inferred from a_1 through a_{35} using modes with $160 \le l \le 250$. The solution is shown as a function of the target latitude. The solid lines from bottom to top are for each time period. For clarity, lines are offset by 1 nHz per 72 days. The dashed lines around the results for the first time interval indicate the 1 σ errors as propagated from the input error estimates. The errors are similar for the other times.

close to the pole. Both of these features are further illustrated in Figure 5.

The evolution of the polar rotation rate is illustrated in Figure 6 for a number of latitudes. Again, the temporal evolution is obvious for latitudes above 70°. It should, of course, be noted that the latitude resolution is quite limited and that the rotation rates shown are thus rather broad averages.

3. DISCUSSION

It is clear that there is a very strong small-scale zonal flow signal in the MDI f-mode frequency splittings. This is consistent with the results reported by Kosovichev & Schou (1997), Schou et al. (1998a, 1998b), and Birch & Kosovichev (1998a, 1998b). Furthermore, it is seen that the narrow bands of faster and slower rotation migrate toward the equator in a manner similar to that seen in surface Doppler shift measurements or in the latitudes of the appearance of sunspots. Indeed, it has been noted that the latitudes of the emergence of sunspots appear to follow closely one of the features in the zonal flows. The physical significance of this is not clear.

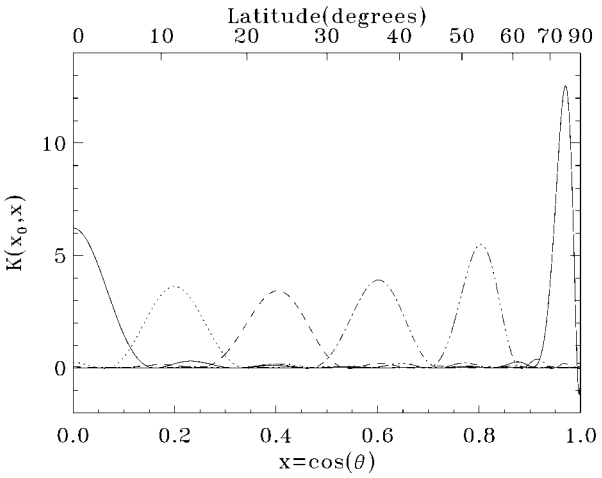

FIG. 4.—Averaging kernels in latitude for target x_0 = 0.0, 0.2, 0.4, 0.6, 0.8, and 0.965 (corresponding to a latitude of 75°).

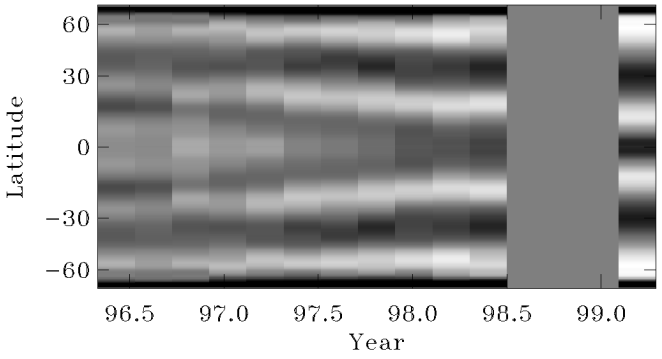

FIG. 5.—The zonal flows from Fig. 3 shown as a function of time and latitude. White corresponds to a prograde velocity of 7 m s^{-1}, while black corresponds to −7 m s^{-1}. The vertical axis is evenly spaced in sin (latitude).

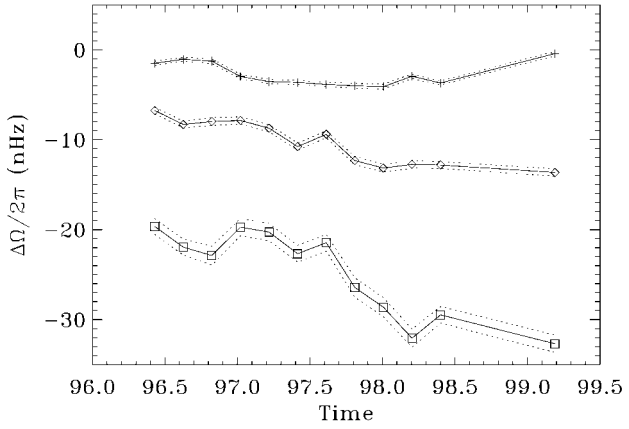

FIG. 6.—The rotation rate at various latitudes as a function of time. From top to bottom, target x_0 of sin (70°) (*crosses*), sin (75°) (*diamonds*), and sin (80°) (*squares*), corresponding to centers of gravity of sin (68.°7), sin (73.°3), and sin (78.°2), respectively. The dotted lines indicate 1 σ errors.

It is interesting to note that the contrast of the features seems to be increasing with time. Again, the cause is not obvious, but it may simply be related to the increase in spacing between the bands and the disappearance of a band at the equator during the time period studied. Also, there are significant deviations from the simple picture of bands migrating toward the equator (perhaps most obvious in Fig. 3 around 60° latitude). It remains to be seen from further analysis of MDI and other data sets whether these deviations are real or due to systematic or random errors in the data. If real, they may help shed light on the origin of the bands and the properties of large-scale patterns in the turbulent convection in the Sun's convective envelope.

In Schou et al. (1998b), the radial extent of the zonal flows was estimated to be at least 1%–2% and possibly up to 5% using both *p*- and *f*-modes. With more and/or longer data sets (and thereby lower noise), it should be possible to estimate the radial extent better and to look for any other structures, as well as to characterize the temporal evolution better. In particular, it may be of interest to determine whether the structures are largely radial or cylindrical since this may help constrain models of angular momentum transport in the convection zone.

It is interesting to note that the rotation rate near the poles is very slow, as noticed by Schou et al. (1998b) and Birch & Kosovichev (1998a, 1998b). From Figure 6, it is clear that there are significant changes in this rotation rate. Similar changes have been reported from surface measurements. Given the widths of the averaging kernels, the change from small deviations from the simple extrapolation to the slow rotation near the poles appears to be quite sharp. The smearing caused by the averaging, however, should not affect the conclusion that the rotation is slow or that it appears to be temporally variable. It appears that the different latitudes shown in Figure 6 have a somewhat different behavior. The next one or two 72 day series should help establish the trends and, in particular, determine when the rotation rate at the highest latitudes starts increasing. Also, it should eventually be possible to determine if the variations in the polar rotation rate are consistent with Birch & Kosovichev (1998b). The physical significance of the polar flow variations and their relation to the zonal flows and other features like polar fields is not clear. Again, more and longer time series should help.

The present analysis used MDI data. The Global Oscillation Network Group (GONG) instrument may be able to provide data slightly earlier and during the gap in the MDI data (during which there is a stretch of possibly useful MDI data). Unfortunately, the current GONG analysis only goes up to $l = 200$ because of aliasing problems. This severely limits the number of useful modes, but experiments indicate that there is still useful information below this limit. For obtaining an even longer time base, possibly covering a solar cycle, it may be interesting to use data from other experiments such as LOWL or Mount Wilson.

The Solar Oscillations Investigation–MDI project is supported by NASA grant NAG5-3077 to Stanford University. *SOHO* is a mission of international cooperation between ESA and NASA.

REFERENCES

Birch, A. C., & Kosovichev, A. G. 1998a, ApJ, 503, L187
———. 1998b, in Proc. *SOHO* 6/GONG 98 Workshop, Structure and Dynamics of the Interior of the Sun and Sun-like Stars, ed. S. Korzennik & A. Wilson (ESA SP-418; Noordwijk: ESA), 679
Christensen-Dalsgaard, J., Schou, J., & Thompson, M. J. 1990, MNRAS, 242, 353
Howard, R., & LaBonte, B. J. 1980, ApJ, 239, L33
Kosovichev, A. G., & Schou, J. 1997, ApJ, 482, L207
Pijpers, F. P. 1997, A&A, 326, 1235
Schou, J. 1992, Ph.D. thesis, Aarhus Univ.
Schou, J., Christensen-Dalsgaard, J., & Thompson, M. J. 1994, ApJ, 433, 389
Schou, J., et al. 1998a, in IAU Symp. 185, New Eyes to See inside the Sun and Stars: Pushing the Limits of Helio- and Asteroseismology with New Observations from the Ground and from Space, ed. F.-L. Deubner, J. Christensen-Dalsgaard, & D. Kurtz (Dordrecht: Kluwer), 141
———. 1998b, ApJ, 505, 390